



CO₂-dependent carbon isotope fractionation in dinoflagellates relates to their inorganic carbon fluxes



Mirja Hoins^{a,b,*}, Tim Eberlein^b, Dedmer B. Van de Waal^c, Appy Sluijs^a, Gert-Jan Reichart^{a,d}, Björn Rost^b

^a Department of Earth Sciences, Faculty of Geosciences, Utrecht University, Budapestlaan 4, 3584 CD Utrecht, The Netherlands

^b Marine Biogeosciences, Alfred Wegener Institute, Helmholtz Centre for Polar- and Marine Research, Am Handelshafen 12, 27570 Bremerhaven, Germany

^c Department of Aquatic Ecology, Netherlands Institute of Ecology (NIOO-KNAW), Droevendaalsesteeg 10, 6708 PB Wageningen, The Netherlands

^d Royal Netherlands Institute for Sea Research (NIOZ), Landsdiep 4, 1797 SZ 't Horntje, Texel, The Netherlands

ARTICLE INFO

Article history:

Received 12 September 2015

Received in revised form 3 April 2016

Accepted 4 April 2016

Available online 30 April 2016

Keywords:

CCM

CO₂ uptake

HCO₃⁻ uptake

Leakage

ABSTRACT

Carbon isotope fractionation (ϵ_p) between the inorganic carbon source and organic matter has been proposed to be a function of $p\text{CO}_2$. To understand the CO₂-dependency of ϵ_p and species-specific differences therein, inorganic carbon fluxes in the four dinoflagellate species *Alexandrium fundyense*, *Scrippsiella trochoidea*, *Gonyaulax spinifera* and *Protoceratium reticulatum* have been measured by means of membrane-inlet mass spectrometry. In-vivo assays were carried out at different CO₂ concentrations, representing a range of $p\text{CO}_2$ from 180 to 1200 μatm . The relative bicarbonate contribution (i.e. the ratio of bicarbonate uptake to total inorganic carbon uptake) and leakage (i.e. the ratio of CO₂ efflux to total inorganic carbon uptake) varied from 0.2 to 0.5 and 0.4 to 0.7, respectively, and differed significantly between species. These ratios were fed into a single-compartment model, and ϵ_p values were calculated and compared to carbon isotope fractionation measured under the same conditions. For all investigated species, modeled and measured ϵ_p values were comparable (*A. fundyense*, *S. trochoidea*, *P. reticulatum*) and/or showed similar trends with $p\text{CO}_2$ (*A. fundyense*, *G. spinifera*, *P. reticulatum*). Offsets are attributed to biases in inorganic flux measurements, an overestimated fractionation factor for the CO₂-fixing enzyme RubisCO, or the fact that intracellular inorganic carbon fluxes were not taken into account in the model. This study demonstrates that CO₂-dependency in ϵ_p can largely be explained by the inorganic carbon fluxes of the individual dinoflagellates.

© 2016 The Authors. Published by Elsevier B.V. This is an open access article under the CC BY license (<http://creativecommons.org/licenses/by/4.0/>).

1. Introduction

During photosynthetic carbon fixation, the lighter carbon isotope ¹²C is preferred over the heavier carbon isotope ¹³C, thereby causing carbon isotope fractionation (ϵ_p) between the inorganic carbon (C_i) source and the organic carbon. Values for ϵ_p of marine phytoplankton have been shown to be CO₂-sensitive (e.g. Degens et al., 1968), and thus were discussed to serve as a proxy for past CO₂ concentrations (Jasper and Hayes, 1990; Pagani, 2014; Van de Waal et al., 2013; Hoins et al., 2015). Large species-specific differences in ϵ_p have been

described, which are yet poorly understood (e.g. Hinga et al., 1994; Burkhardt et al., 1999). Moreover, irrespective of the phytoplankton species investigated, most of these studies have solely described the relationship between ϵ_p and CO₂, and only few have investigated the underlying physiological processes. Such mechanistic understanding is, however, needed to identify the reasons of the CO₂-dependency of ϵ_p .

Carbon isotope fractionation of phytoplankton is primarily driven by the enzyme ribulose-1,5-bisphosphate Carboxylase/Oxygenase (RubisCO), which is responsible for the fixation of CO₂ into organic compounds. The intrinsic fractionation associated with RubisCO (ϵ_f) has been estimated to range between ~22 and 30‰ (e.g. Roeske and O'Leary, 1984; Guy et al., 1993; Scott et al., 2007), even though a recent study obtained values as low as 11‰ for the RubisCO of the coccolithophore *Emiliania huxleyi* (Boller et al., 2011). While RubisCO principally sets the upper limit of fractionation, other processes strongly determine the degree to which RubisCO can express its fractionation (Sharkey and Berry, 1985; Burkhardt et al., 1999; Rost et al., 2002). First, there is leakage, i.e. the amount of CO₂ diffusing out of the cell in relation to C_i uptake. With higher leakage, the intracellular C_i pool is 'refreshed', thereby preventing accumulation of ¹³C and allowing RubisCO to approach its upper fractionation values. Second, the relative

Abbreviations: C_i, inorganic carbon; CCM, CO₂-concentrating mechanism; Chl-*a*, Chlorophyll-*a*; ϵ_p , carbon isotope fractionation; $\epsilon_{p\text{-meas}}$, measured carbon isotope fractionation; $\epsilon_{p\text{-mod}}$, modeled carbon isotope fractionation; ϵ_s , equilibrium fractionation between CO₂ and HCO₃⁻; ϵ_f , kinetic fractionation associated with the CO₂ fixation of RubisCO; L_{CO₂}, ratio of CO₂ efflux relative to total C_i uptake; DIC, dissolved inorganic carbon; HCO₃⁻, bicarbonate; R_{HCO₃}, ratio of HCO₃⁻ to total C_i uptake; RubisCO, ribulose-1,5-bisphosphate Carboxylase/Oxygenase; CA, carbonic anhydrase; TA, total alkalinity.

* Corresponding author at: Department of Earth Sciences, Faculty of Geosciences, Utrecht University, Budapestlaan 4, 3584 CD Utrecht, The Netherlands.

E-mail addresses: mhoins@awi.de (M. Hoins), tim.eberlein@awi.de (T. Eberlein),

D.vandeWaal@nioo.knaw.nl (D.B. Van de Waal), a.sluijs@uu.nl (A. Sluijs),

g.j.reichart@uu.nl (G.-J. Reichart), bjoern.rost@awi.de (B. Rost).

contribution of bicarbonate (HCO_3^-) to total C_i uptake plays a role, as HCO_3^- is enriched in ^{13}C by ~10‰ relative to CO_2 (Mook et al., 1974). An increasing HCO_3^- contribution thus lowers ϵ_p . The enzyme carbonic anhydrase (CA), which accelerates the otherwise slow interconversion between CO_2 and HCO_3^- , can also influence ϵ_p under certain conditions, e.g. by influencing leakage as well as the relative HCO_3^- contribution. All these processes play a role in the CO_2 -concentrating mechanisms (CCMs) of phytoplankton. Assessing the mode of CCMs may therefore help to understand the reasons for CO_2 -dependent changes in ϵ_p and species-specific differences therein.

Dinoflagellates are cosmopolitan unicellular algae that occur in many different environments, including eutrophic coastal regions and oligotrophic open oceans. In this study, we investigated whether the CO_2 -dependency of ϵ_p , which was found in the dinoflagellate species *Alexandrium fundyense*, *Gonyaulax spinifera*, *Protoceratium reticulatum* and *Scrippsiella trochoidea* (Burkhardt et al., 1999; Hoins et al., 2015), can be explained by changes in their C_i fluxes. Characteristics of CCMs in the tested species, including their CA activities and C_i fluxes, were measured by means of membrane-inlet mass spectrometry (MIMS). Results were fed into a single-compartment model that considers cellular leakage, the relative HCO_3^- contribution as well as the carbon isotope fractionation of RubisCO (Sharkey and Berry, 1985; Burkhardt et al., 1999). The calculated carbon fractionation ($\epsilon_{p\text{-mod}}$) was then compared to the measured carbon fractionation ($\epsilon_{p\text{-meas}}$).

2. Material and methods

2.1. Incubations

Cultures of the dinoflagellate species *A. fundyense* (formerly *Alexandrium tamarense* strain Alex5; John et al., 2014), *S. trochoidea* (strain Geob267; culture collection of the University of Bremen), *G. spinifera* (strain CCMP 409) and *P. reticulatum* (strain CCMP 1889) were grown in 0.2 μm filtered North Sea water (salinity 34), which was enriched with 100 $\mu\text{mol L}^{-1}$ nitrate and 6.25 $\mu\text{mol L}^{-1}$ phosphate. Metals and vitamins were added according to f/2 medium (Guillard and Ryther, 1962), except for FeCl_3 (1.9 $\mu\text{mol L}^{-1}$), H_2SeO_3 (10 nmol L^{-1}) and NiCl_2 (6.3 nmol L^{-1}) that were added according to K medium (Keller et al., 1987). Each of the strains was grown in 2.4 L air-tight borosilicate bottles at 15 °C and $250 \pm 25 \mu\text{mol photons m}^{-2} \text{s}^{-1}$ at a 16:8 h light:dark cycle. Bottles were placed on roller tables in order to avoid sedimentation.

Dissolved CO_2 concentrations ranged from ~5–50 $\mu\text{mol L}^{-1}$ and were reached by pre-aerating culture medium with air containing 180, 380, 800 and 1200 $\mu\text{atm pCO}_2$. The carbonate chemistry was calculated based on pH and total alkalinity (TA), using the program CO2sys (Pierrot et al., 2006). pH values were measured using a WTW 3110 pH meter equipped with a SenTix 41 Plus pH electrode (WTW, Weilheim, Germany), which was calibrated prior to measurements to the National Bureau of Standards (NBS) scale. An automated TitroLine burette system (SI Analytics, Mainz, Germany) was used to determine TA. Dissolved inorganic carbon (DIC) was determined colorimetrically using a QuAatro autoanalyser (Seal Analytical, Mequon, USA). For more details on the carbonate chemistry in the acclimations, please refer to Eberlein et al. (2014) for *A. fundyense* and *S. trochoidea* and to Hoins et al. (2015) for *G. spinifera* and *P. reticulatum*.

To determine ϵ_p values, the isotopic composition of the organic material was measured using an Automated Nitrogen Carbon Analyser mass spectrometer (ANCA-SL 20–20, SerCon Ltd., Crewe, UK), and the isotopic composition of the DIC in growth medium was measured using a GasBench-II coupled to a Thermo Delta-V advantage isotope ratio mass spectrometer (see Hoins et al., 2015 for details on isotope analysis). Prior to assays, cells were acclimated to the different CO_2 concentrations for at least 7 generations (i.e. >21 days). To prevent changes in the carbonate chemistry, i.e.

keeping drawdown of DIC <3%, incubations were terminated at low cell densities (<400 cells mL^{-1}).

2.2. MIMS assays

A custom-made membrane-inlet mass spectrometer (MIMS; Isoprime, GV Instruments, Manchester, UK; see Rost et al., 2007 for details) was used to determine CA activities and C_i fluxes of *A. fundyense* and *S. trochoidea* acclimated to four different pCO_2 (i.e. 180, 380, 800 and 1200 μatm ; Eberlein et al., 2014), and of *G. spinifera* and *P. reticulatum* acclimated to a low and high pCO_2 (i.e. 180 and 800 μatm). Assays were performed in an 8 mL temperature-controlled cuvette, equipped with a stirrer. Assay tests over ~1 h confirmed that conditions during the assay do not cause physiological stress (i.e. no decline in O_2 production rates), and subsequent microscopic inspection did not reveal any visual effects on cell morphologies. Prior to the measurements, acclimated cells were concentrated using a 10 μm membrane filter (Millipore, Billerica, MA) by gentle vacuum filtration (<200 mbar) and stepwise transferred into C_i -free medium buffered with a 4-(2-hydroxyethyl)-1-piperazine-ethanesulfonic acid (50 mmol L^{-1} HEPES) solution at 15 ± 0.3 °C and a pH of 8.0 ± 0.1 . Chlorophyll *a* (Chl-*a*) concentrations were determined fluorometrically by using a TD-700 Fluorometer (Turner Designs, Sunnyvale, CA, USA) and ranged between 0.15 and 1.70 $\mu\text{g mL}^{-1}$ during the assays.

To quantify activities of extracellular CA (eCA), the ^{18}O depletion rate of doubly labeled $^{13}\text{C}^{18}\text{O}_2$ in seawater was determined by measuring the transient changes in $^{13}\text{C}^{18}\text{O}^{18}\text{O}$ ($m/z = 49$), $^{13}\text{C}^{18}\text{O}^{16}\text{O}$ ($m/z = 47$) and $^{13}\text{C}^{16}\text{O}^{16}\text{O}$ ($m/z = 45$) in the dark, following the approach of Silvermann (1982). If cells possess eCA, exchange rates of ^{18}O are accelerated relative to the spontaneous rate. To monitor the spontaneous rate, $\text{NaH}^{13}\text{C}^{18}\text{O}_3$ label was injected to the cuvette, waiting until the $m/z = 49$ signal reached a steady-state decline. This rate was then compared to the steady-state decline after cells were added. Following Badger and Price (1989), eCA activity is expressed as percentage decrease in ^{18}O -atom fraction upon the addition of cells, normalized to Chl-*a*. Consequently, 100 units (U) correspond to a doubling in the rate of interconversion between CO_2 and HCO_3^- per $\mu\text{g Chl-}a$.

Photosynthetic O_2 and C_i fluxes were determined following Badger et al. (1994). Making use of the chemical disequilibrium, this approach estimates CO_2 and HCO_3^- fluxes during steady-state photosynthesis. It is based on the simultaneous measurements of O_2 and CO_2 concentrations during consecutive light and dark intervals with increasing amounts of DIC. Oxygen fluxes in the dark and light are converted into C_i fluxes by applying a respiratory quotient of 1.0 and a photosynthetic quotient of 1.1 (Burkhardt et al., 2001; Rost et al., 2003). The light intensity in the cuvette was adjusted to the acclimation conditions (i.e. $250 \pm 25 \mu\text{mol photons m}^{-2} \text{s}^{-1}$). Net CO_2 uptake was calculated from the steady-state decline in CO_2 concentration at the end of the light period, corrected for the interconversion between CO_2 and HCO_3^- . The uptake of HCO_3^- was calculated by subtracting net CO_2 uptake from net C_i uptake, and the CO_2 efflux from the cells was estimated from the initial slope after turning off the light. Rate constants k_1 and k_2 were determined based on temperature, salinity and pH (Zeebe and Wolf-Gladrow, 2001; Schulz et al., 2006), yielding mean values of $0.9241 (\pm 0.0506) \text{ min}^{-1}$ and $0.0085 (\pm 0.0008) \text{ min}^{-1}$, respectively. To eliminate any eCA activity, a prerequisite to apply the rate constants, we added dextran-bound sulfonamide (DBS; 50 $\mu\text{mol L}^{-1}$) to the cuvette. For more details on the calculations, please refer to Badger et al. (1994) and Schulz et al. (2007).

2.3. Single-compartment model

To calculate $\epsilon_{p\text{-mod}}$, results for the relative HCO_3^- contribution and leakage were fed into a single-compartment model after Sharkey and

Berry (1985) and Burkhardt et al. (1999):

$$\epsilon_{p-mod} = R_{HCO_3} \times \epsilon_s + L_{CO_2} \times \epsilon_f \quad (1)$$

where R_{HCO_3} represents the ratio of HCO_3^- to total C_i uptake, ϵ_s the equilibrium fractionation between CO_2 and HCO_3^- (−10‰; Mook et al., 1974), L_{CO_2} the ratio of CO_2 efflux relative to total C_i uptake, and ϵ_f the kinetic fractionation associated with the CO_2 fixation of RubisCO, which was here assumed to be 28‰ after Raven and Johnston (1991).

2.4. Statistical analysis

Shapiro–Wilk tests confirmed normality of the data. Significant differences between CO_2 treatments were confirmed by a one-way ANOVA followed by post hoc comparison of the means using the Tukey HSD ($\alpha = 0.05$; Table 1).

3. Results

3.1. CA activity

In *A. fundyense* and *P. reticulatum*, eCA activities were low with maximum activities of 156 U ($\mu\text{g Chl-}a^{-1}$) and 44 U ($\mu\text{g Chl-}a^{-1}$), respectively. In *S. trochoidea* and *G. spinifera*, eCA activities were comparably high with up to 1600 U ($\mu\text{g Chl-}a^{-1}$) and 1100 U ($\mu\text{g Chl-}a^{-1}$), respectively. In neither of the species, eCA activities were responding to changes in pCO_2 . Please note that for *G. spinifera* and *P. reticulatum* no statistics could be applied due to the lack of replication.

3.2. HCO_3^- contribution and leakage

Relative HCO_3^- contribution was around 0.2 in *A. fundyense* and *G. spinifera* (Figs. 1A and 3A; Table 1), whereas *S. trochoidea* and *P. reticulatum* showed higher values of ~0.5 (Figs. 2A and 4A; Table 1). In other words, in *A. fundyense* and *G. spinifera* approximately 80% of the C_i taken up is in the form of CO_2 , whereas in *S. trochoidea* and *P. reticulatum* this was 50%. There was a significant decrease in HCO_3^- contribution with increasing CO_2 concentration in *S. trochoidea*, while

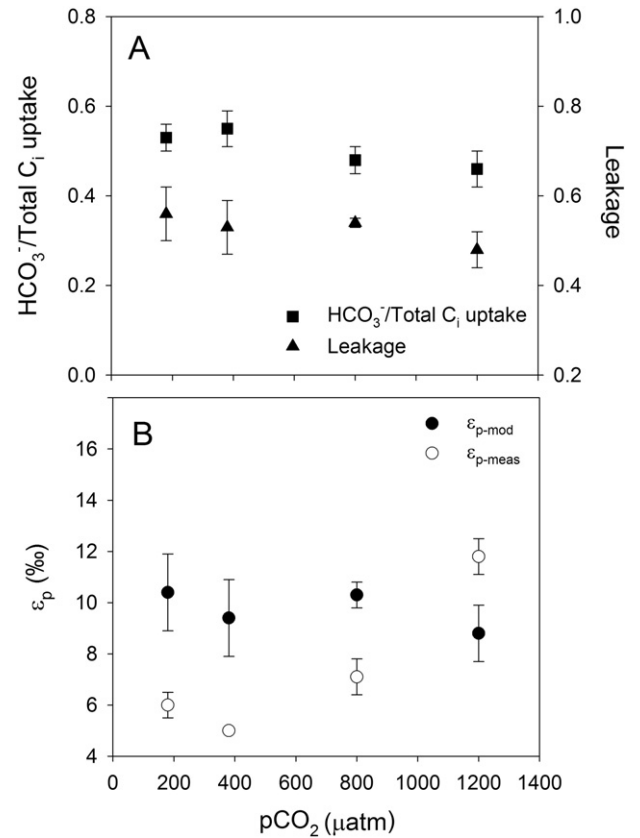


Fig. 1. Relative HCO_3^- contribution, leakage and ϵ_{p-mod} and ϵ_{p-meas} in *A. fundyense*. Each data point represents the mean \pm standard deviation ($n = 3$).

no such CO_2 -dependency was observed in any of the other tested species. Leakage differed significantly between the tested species, with values of up to 0.7 at 800 $\mu\text{atm } pCO_2$ in *G. spinifera* (Fig. 3A; Table 1) and lowest average values of ~0.5 in *S. trochoidea* and *P. reticulatum*,

Table 1

Experimental conditions in dilute batch culture incubations (see also Eberlein et al., 2014; Hoins et al., 2015): average CO_2 concentrations ($\mu\text{mol L}^{-1}$), total alkalinity (TA; $\mu\text{mol L}^{-1}$), dissolved inorganic carbon (DIC; $\mu\text{mol L}^{-1}$) and pH (NBS scale). HCO_3^- contribution, leakage, modeled carbon isotope fractionation (ϵ_{p-mod}) and measured carbon isotope fractionation (ϵ_{p-meas}) was derived under the same conditions.

pCO_2 μatm	CO_2 $\mu\text{mol L}^{-1}$	TA $\mu\text{mol L}^{-1}$	DIC $\mu\text{mol L}^{-1}$	pH NBS	HCO_3^- contribution	Leakage	ϵ_{p-mod} ‰	ϵ_{p-meas} ‰
<i>A. fundyense</i>								
180	5.9 \pm 0.9 ^a	2434 \pm 3	1992 \pm 10 ^a	8.50 \pm 0.06 ^a	0.22 \pm 0.03	0.44 \pm 0.01 ^a	10.1 \pm 0.2 ^a	9.0 \pm 0.3 ^a
380	11.5 \pm 2.1 ^b	2439 \pm 1	2117 \pm 8 ^b	8.27 \pm 0.07 ^b	0.24 \pm 0.04	0.46 \pm 0.02 ^a	10.6 \pm 0.5 ^a	10.2 \pm 0.5 ^b
800	25.9 \pm 5.8 ^c	2434 \pm 2	2245 \pm 8 ^c	7.97 \pm 0.10 ^c	0.24 \pm 0.04	0.53 \pm 0.02 ^b	12.6 \pm 0.6 ^b	12.7 \pm 0.4 ^c
1200	36.5 \pm 9.3 ^d	2418 \pm 1	2283 \pm 5 ^d	7.83 \pm 0.12 ^d	0.23 \pm 0.08	0.63 \pm 0.05 ^c	15.3 \pm 0.8 ^c	12.1 \pm 0.2 ^c
<i>S. trochoidea</i>								
180	6.6 \pm 0.2 ^a	2386 \pm 1	1872 \pm 2 ^a	8.45 \pm 0.01 ^a	0.53 \pm 0.03 ^{ab}	0.56 \pm 0.06	10.4 \pm 1.5	6.0 \pm 0.5 ^{a,b}
380	13.1 \pm 0.5 ^b	2388 \pm 2	2096 \pm 3 ^b	8.21 \pm 0.02 ^b	0.55 \pm 0.04 ^a	0.53 \pm 0.06	9.4 \pm 1.5	5.0 \pm 0.1 ^a
800	28.8 \pm 2.0 ^c	2385 \pm 1	2223 \pm 3 ^c	7.91 \pm 0.03 ^c	0.48 \pm 0.03 ^{b,c}	0.54 \pm 0.01	10.3 \pm 0.5	7.1 \pm 0.7 ^b
1200	41.5 \pm 3.6 ^d	2386 \pm 4	2268 \pm 9 ^d	7.77 \pm 0.04 ^d	0.46 \pm 0.04 ^c	0.48 \pm 0.04	8.8 \pm 1.1	11.8 \pm 0.7 ^c
<i>G. spinifera</i>								
180	6.0 \pm 1.1 ^a	2447 \pm 5	1962 \pm 15 ^a	8.50 \pm 0.05 ^a	0.19 \pm 0.11	0.61 \pm 0.01	15.6 \pm 0.9 ^a	7.8 \pm 1.0 ^a
380	11.7 \pm 2.5 ^b	2461 \pm 12	2083 \pm 1 ^b	8.27 \pm 0.07 ^b	–	–	–	9.4 \pm 0.4 ^a
800	27.9 \pm 7.4 ^c	2475 \pm 13	2224 \pm 9 ^c	7.96 \pm 0.10 ^c	0.19 \pm 0.11	0.71 \pm 0.01	18.6 \pm 1.7 ^b	11.7 \pm 0.7 ^b
1200	42.4 \pm 7.9 ^d	2459 \pm 4	2293 \pm 5 ^d	7.78 \pm 0.06 ^d	–	–	–	8.1 \pm 0.5 ^a
<i>P. reticulatum</i>								
180	7.1 \pm 0.5 ^a	2460 \pm 8	2002 \pm 2 ^a	8.43 \pm 0.04 ^a	0.44 \pm 0.13	0.50 \pm 0.06	9.58 \pm 2.0	8.4 \pm 1.8
380	13.9 \pm 0.8 ^b	2455 \pm 2	2121 \pm 4 ^b	8.21 \pm 0.02 ^b	–	–	–	8.4 \pm 0.7
800	31.0 \pm 4.7 ^c	2461 \pm 12	2249 \pm 23 ^c	7.88 \pm 0.08 ^c	0.49 \pm 0.19	0.48 \pm 0.09	9.2 \pm 1.9	8.6 \pm 2.0
1200	45.2 \pm 6.9 ^d	2473 \pm 19	2288 \pm 16 ^d	7.75 \pm 0.05 ^d	–	–	–	9.9 \pm 0.8

Values represent the mean of triplicate incubations ($n = 3$; \pm SD). Superscript letters indicate significant differences between pCO_2 treatments ($P < 0.05$).

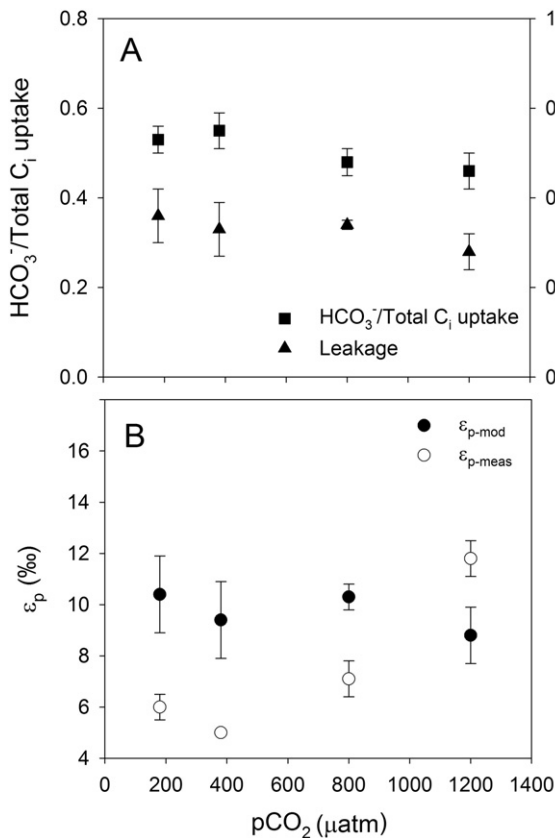


Fig. 2. A) Relative HCO₃⁻ contribution, leakage and B) ε_{p-mod} and ε_{p-meas} in *S. trochoidea*. Each data point represents the mean ± standard deviation (n = 3).

respectively (Figs. 2A and 4A; Table 1). Only in *A. fundyense*, leakage was significantly CO₂-dependent and increased from 0.44 to 0.63 (Fig. 1A; Table 1). For details on the kinetics of O₂, CO₂ and HCO₃⁻ fluxes in *A. fundyense* and *S. trochoidea*, please refer to Eberlein et al. (2014).

3.3. C_i flux based ε_p calculations

Estimates for ε_{p-mod} are in the same range as ε_{p-meas} in *A. fundyense* and *P. reticulatum* (Figs. 1B and 4B; Table 1), while the model overestimated the fractionation by up to 5‰ and 8‰ in *S. trochoidea* and *G. spinifera*, respectively (Figs. 2B and 3B; Table 1). Except for *S. trochoidea*, ε_{p-mod} generally matches trends observed in ε_{p-meas}. In *A. fundyense*, for instance, ε_{p-mod} increased significantly from 10.1 to 15.3‰, thereby closely matching ε_{p-meas} values (Fig. 1B; Table 1). Also in *G. spinifera*, ε_{p-mod} matches trends observed in ε_{p-meas}, if the highest pCO₂ treatment of ε_{p-meas} is excluded. In this treatment, carbon isotope fractionation dropped significantly, most likely due to 2.5-fold increased cellular carbon contents (see discussion in Hoins et al., 2015). In *S. trochoidea*, neither the relative HCO₃⁻ contribution nor leakage showed a CO₂-dependency; hence ε_{p-mod} did not match the increase in ε_{p-meas} with increasing CO₂ concentration (Fig. 2B; Table 1).

4. Discussion

4.1. CA activity plays a minor role in C_i fluxes

By expressing CA, many marine algae species accelerate the otherwise slow interconversion between CO₂ and HCO₃⁻, thereby possibly facilitating the C_i uptake and internal C_i fluxes. In line with previous studies on dinoflagellates (Rost et al., 2006; Ratti et al., 2007), *A. fundyense* and *P. reticulatum* exhibit rather low eCA activities, even under low CO₂ concentrations. In view of this, eCA is not expected to

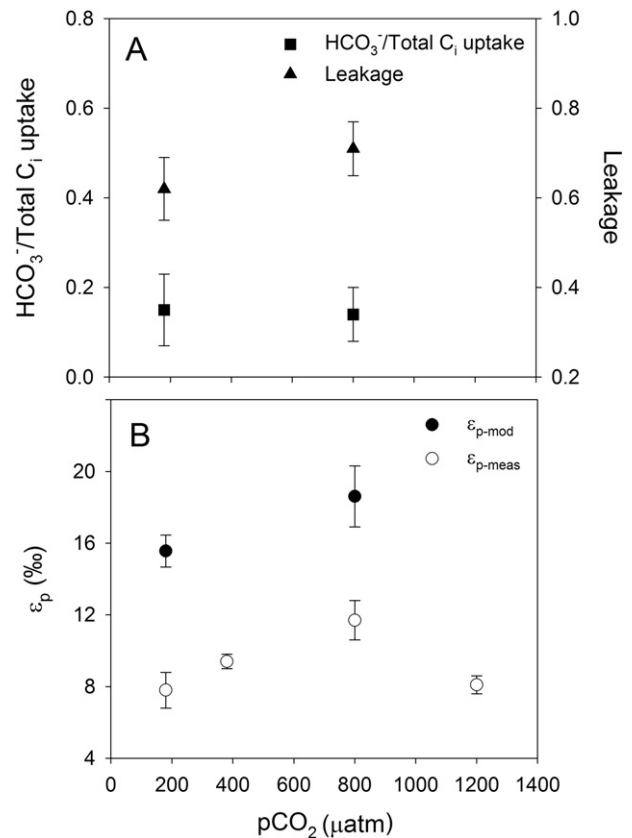


Fig. 3. A) Relative HCO₃⁻ contribution, leakage and B) ε_{p-mod} and ε_{p-meas} in *G. spinifera*. Each data point represents the mean ± standard deviation (n = 3).

significantly influence C_i fluxes or ε_p in these species. In *S. trochoidea* and *G. spinifera*, however, eCA activities were high at all tested CO₂ concentrations, comparable to values observed for temperate diatoms (Trimborn et al., 2009). Hence, the inhibition of eCA by the inhibitor DBS during the MIMS assay might have biased the C_i fluxes, i.e. underestimated CO₂ uptake (Rost et al., 2003), thereby potentially causing an underestimation of ε_p. As these were the species for which the model overestimated ε_p values, however, it can be concluded that eCA (and its inhibition by DBS during the C_i flux measurements) did not influence the C_i fluxes much.

4.2. Species-specific differences in C_i fluxes

The HCO₃⁻ contribution differed considerably between the tested species. While *A. fundyense* and *G. spinifera* showed a strong preference for CO₂, *S. trochoidea* and *P. reticulatum* used CO₂ and HCO₃⁻ in equal proportions. The latter contradicts with the findings of an endpoint pH-drift experiment, suggesting that *P. reticulatum* is not able to efficiently use HCO₃⁻ (Ratti et al., 2007). Testing other dinoflagellates with a modified pH-drift method, including the genus *Protoceratium*, demonstrated that the high pH itself can affect growth and thus interpretations about the used C_i source based on pH-drift experiments must be considered with caution (Hansen et al., 2007). From an energetic point of view, high CO₂ usage would be of advantage as CO₂ can be taken up passively by diffusion, while HCO₃⁻ is charged and thus has to be taken up by active uptake. And yet, the tested species covered a large part of their C_i demand by HCO₃⁻, as observed in *S. trochoidea* and *P. reticulatum* (Figs. 2A and 4A).

Similarly high HCO₃⁻ contributions were observed for other dinoflagellate species (Rost et al., 2006) and cyanobacteria (Price et al., 2008; Kranz et al., 2011). This preference for HCO₃⁻ has been associated with the very low CO₂-affinity of RubisCO type IB, which is expressed

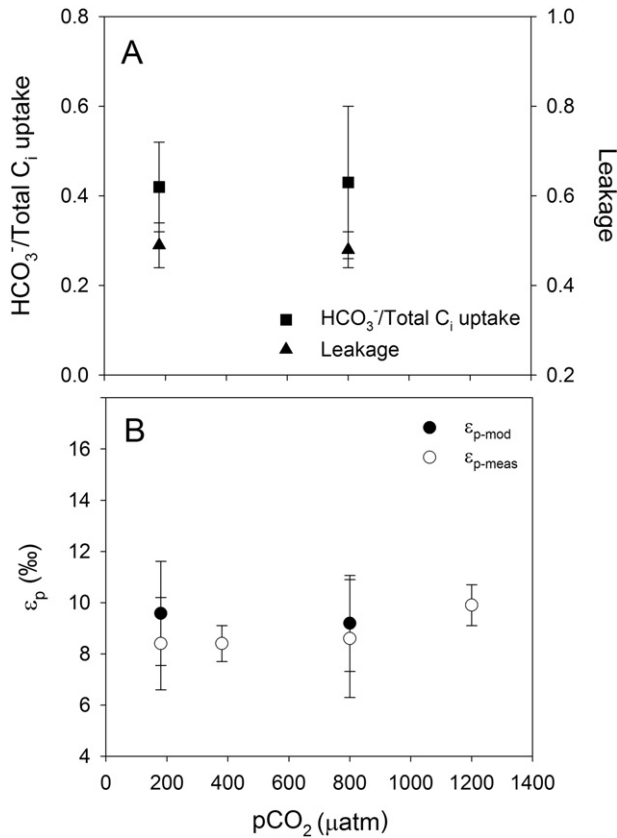


Fig. 4. A) Relative HCO₃⁻ contribution, leakage and B) ε_{p-mod} and ε_{p-meas} in *P. reticulatum*. Each data point represents the mean ± standard deviation (n = 3).

in cyanobacteria, and RubisCO type II expressed in dinoflagellates (Badger et al., 1998; Whitney and Andrews, 1998). To compensate for this low affinity, high amounts of C_i have to be accumulated, which in seawater can more easily be accomplished with the abundant HCO₃⁻ ion rather than with CO₂. In addition, HCO₃⁻ is about 1000-fold less permeable to lipid membranes than CO₂, making it the preferred C_i form to be accumulated within the cell (Price et al., 2008). In the case where species covered the majority of their C_i demand by CO₂, as observed in *A. fundyense* and *G. spinifera* (Figs. 1A and 3A), one could therefore speculate about chloroplast-based C_i accumulation rather than pumping of HCO₃⁻ at the cell wall (Badger et al., 1998). The observed differences in the preferred C_i source and likely consequences for internal C_i fluxes may also affect the overall leakage of cells.

Also leakage differed considerably among the species. *A. fundyense* showed a relatively low leakage of 0.44 at 180 μatm pCO₂, which increased to 0.63 at 1200 μatm pCO₂. Leakage in *G. spinifera* varied between 0.60 at 180 μatm pCO₂ and 0.70 at 800 μatm pCO₂. Leakage estimates in *S. trochoidea* and *P. reticulatum* were lower with ~0.50 and remained constant over the applied range of pCO₂. These differences may be caused by different membrane permeabilities, which again potentially relate to the preferred C_i source. In fact, *A. fundyense* and *G. spinifera* both preferred CO₂ over HCO₃⁻ and likewise showed the highest degrees of leakage, thereby suggesting highly permeable membranes with respect to CO₂. In these species, also CO₂-related changes in the membrane permeability are indicated as they show significantly increased leakage under higher pCO₂ (see also Eberlein et al., 2014 for *A. fundyense*, formerly *A. tamarensis*).

4.3. Patterns in carbon isotope fractionation can be explained by C_i fluxes

Using results for HCO₃⁻ contribution and leakage obtained in this study, carbon isotope fractionation was calculated and compared to

previous measurements (Figs. 1B–4B; see also Hoins et al., 2015). Generally, there is a good agreement as ε_{p-mod} and ε_{p-meas} values were in the same range (*A. fundyense*, *S. trochoidea*, *P. reticulatum*) and/or followed the same trend (*A. fundyense*, *G. spinifera*, *P. reticulatum*; Figs. 1B–4B). Despite the overall agreement between flux-based estimates and directly measured carbon isotope fractionation, ε_{p-mod} was overestimated in *S. trochoidea* and *G. spinifera*. Such offsets could principally be attributed to biases in the C_i flux measurements, i.e. uncertainties in the estimation of HCO₃⁻ contribution and/or leakage. It has been argued, however, that the MIMS approach tends to overestimate the HCO₃⁻ contribution (due to the constant pH of 8.0 during the assay, see Burkhardt et al., 2001), and rather underestimates cellular leakage (due to fact that CO₂ fixation does not cease instantly upon darkening, see Badger et al., 1994). Hence, by correcting for these potential biases, i.e. assuming slightly lower HCO₃⁻ contribution and higher leakage values, we would actually overestimate the fractionation even more for *S. trochoidea* and *G. spinifera*.

An alternative explanation for the overestimation by the model may be attributed to the fractionation factor of RubisCO, which we assumed to be 28‰ (Raven and Johnston, 1991). Recent studies have found lower values, even as low as 11‰ as in the case of the coccolithophore *Emiliania huxleyi* (Boller et al., 2011). Even though there are no indications for such low fractionation values in the highly conserved type II RubisCO, a lower fractionation would bring modeled and measured ε_p values closer in *S. trochoidea* and *G. spinifera*. In *A. fundyense* and *P. reticulatum*, however, it would lead to underestimated ε_{p-mod}. Hence, we would refrain from assuming much lower fractionation values for RubisCO type II in dinoflagellates in our calculations. Lastly, the fact that internal C_i fluxes were not taken into account might have also contributed to the offsets between ε_{p-mod} and ε_{p-meas}. Models that incorporate internal C_i cycling have, however, caused even higher ε_{p-mod}, as these processes work against the ¹³C accumulation within the chloroplasts (Cassar et al., 2006; Schulz et al., 2007) or the carboxysome (Eichner et al., 2015). Therefore, although the values and trends in carbon isotope fractionation are relatively well understood based on our physiological experiments, differences between theory and measurements are at present not fully resolved.

5. Conclusions

Our study demonstrates that carbon isotope fractionation in dinoflagellates can, to a large degree, be explained by considering their C_i fluxes. Relative HCO₃⁻ contribution and/or leakage were CO₂-dependent in *A. fundyense*, *S. trochoidea* and *G. spinifera*, which in turn can explain the CO₂-dependency of their ε_p observed in previous studies (Hoins et al., 2015). To further advance our understanding of the ε_p patterns in dinoflagellates, C_i fluxes measurements should be performed at in situ pH (Kottmeier et al., 2014, 2016) and ideally differentiate between ¹³C and ¹²C fluxes (McNevin et al., 2006).

Acknowledgments

This research was funded through the Darwin Centre for Biogeosciences Grant 3021, awarded to GJR and AS, and the European Research Council under the Seventh Framework Program of the European Community through ERC Starting Grants #259627 to AS and #205150 to BR. DBvdW and BR thank BIOACID, financed by the German Ministry of Education and Research. This work was carried out under the program of the Netherlands Earth System Science Centre (NESSC). We thank Urban Tillmann (Alfred Wegener Institute) and Karin Zonneveld (Marum, Bremen University) for providing the dinoflagellate species *Alexandrium fundyense* Alex5 and *Scrippsiella trochoidea* Geob267, respectively, and Ulrike Richter, Laura Wischniewski, Jana Hölscher (Alfred Wegener Institute) and Arnold van Dijk (Utrecht University) for technical support. [SS]

References

- Badger, M.R., Price, G.D., 1989. Carbonic anhydrase activity associated with the cyanobacterium *Synechococcus* PCC7942. *Plant Physiol.* 89 (1), 51–60.
- Badger, M.R., Palmqvist, K., Yu, J.W., 1994. Measurement of CO₂ and HCO₃⁻ fluxes in cyanobacteria and microalgae during steady-state photosynthesis. *Physiol. Plant.* 90 (3), 529–536.
- Badger, M.R., Andrews, T.J., Whitney, S.M., Ludwig, M., Yellowlees, D.C., Leggat, W., Price, G.D., 1998. The diversity and coevolution of RubisCO, plastids, pyrenoids, and chloroplast-based CO₂-concentrating mechanisms in algae. *Can. J. Bot.* 76 (6), 1052–1071.
- Boller, A.J., Thomas, P.J., Cavanaugh, C.M., Scott, K.M., 2011. Low stable carbon isotope fractionation by coccolithophore RubisCO. *Geochim. Cosmochim. Acta* 75 (22), 7200–7207.
- Burkhardt, S., Riebesell, U., Zondervan, I., 1999. Effects of growth rate, CO₂ concentration, and cell size on the stable carbon isotope fractionation in marine phytoplankton. *Geochim. Cosmochim. Acta* 63, 3729–3741.
- Burkhardt, S., Amoroso, G., Riebesell, U., Sültemeyer, D., 2001. CO₂ and HCO₃⁻ uptake in marine diatoms acclimated to different CO₂ concentrations. *Limnol. Oceanogr.* 46 (6), 1378–1391.
- Cassar, N., Laws, E.A., Popp, B.N., 2006. Carbon isotopic fractionation by the marine diatom *Phaeodactylum tricornutum* under nutrient- and light-limited growth conditions. *Geochim. Cosmochim. Acta* 70 (21), 5323–5335.
- Degens, E.T., Behrendt, M., Gotthardt, B., Reppmann, E., 1968. Metabolic fractionation of carbon isotopes in marine plankton—II. Data on samples collected off the coasts of Peru and Ecuador. *Deep Sea Res. Oceanogr. Abstr.* 15 (1), 11–20.
- Eberlein, T., Van de Waal, D.B., Rost, B., 2014. Differential effects of ocean acidification on carbon acquisition in two bloom-forming dinoflagellate species. *Physiol. Plant.* <http://dx.doi.org/10.1111/pp1.12137>.
- Eichner, M., Thoms, S., Kranz, S.A., Rost, B., 2015. Cellular inorganic carbon fluxes in *Trichodesmium*: a combined approach using measurements and modelling. *J. Exp. Bot.* 66 (3), 749–759.
- Guillard, R.R.L., Ryther, J.H., 1962. Studies of marine planktonic diatoms. I. *Cyclotella nana* Hustedt and *Detonula confervacea* (Cleve) Gran. *Can. J. Microbiol.* 8, 229–239.
- Guy, R.D., Fogel, M.L., Berry, J.A., 1993. Photosynthetic fractionation of the stable isotopes of oxygen and carbon. *Plant Physiol.* 101 (1), 37–47.
- Hansen, P.J., Lundholm, N., Rost, B., 2007. Growth limitation in marine red-tide dinoflagellates: effects of pH versus inorganic carbon availability. *Mar. Ecol. Prog. Ser.* 334, 63–71.
- Hinga, K.R., Arthur, M.A., Pilson, M.E., Whitaker, D., 1994. Carbon isotope fractionation by marine phytoplankton in culture: the effects of CO₂ concentration, pH, temperature, and species. *Glob. Biogeochem. Cycles* 8, 91–102.
- Hoins, M., Van de Waal, D.B., Eberlein, T., Reichart, G.-J., Rost, B., Slujs, A., 2015. Stable carbon isotope fractionation of organic cyst-forming dinoflagellates: evaluating the potential for a CO₂ proxy. *Geochim. Cosmochim. Acta* 160, 267–276.
- Jasper, J.P., Hayes, J.M., 1990. A carbon isotope record of CO₂ levels during the late quaternary. *Nature* 347 (6292), 462–464.
- John, U., Litaker, R.W., Montresor, M., Murray, S., Brosnahan, M.L., Anderson, D.M., 2014. Formal revision of the *Alexandrium tamarense* species complex (*Dinophyceae*) taxonomy: the introduction of five species with emphasis on molecular-based (rDNA) classification. *Protist* 165, 779–804.
- Keller, M.D., Selvin, R.C., Claus, W., Guillard, R.R.L., 1987. Media for the culture of oceanic ultraplankton. *J. Phycol.* 23, 633–638.
- Kottmeier, D.M., Rokitta, S.D., Tortell, P.D., Rost, B., 2014. Strong shift from HCO₃⁻ to CO₂ uptake in *Emiliana huxleyi* with acidification: new approach unravels acclimation versus short-term pH effects. *Photosynth. Res.* 121 (2–3), 265–275.
- Kottmeier, D.M., Rokitta, S.D., Rost, B., 2016. Acidification, not carbonation, is the major regulator of carbon fluxes in the coccolithophore *Emiliana huxleyi*. *New Phytol.* <http://dx.doi.org/10.1111/nph.13885>.
- Kranz, S.A., Eichner, M., Rost, B., 2011. Interactions between CCM and N₂ fixation in *Trichodesmium*. *Photosynth. Res.* 109 (1–3), 73–84.
- McNevin, D.B., Badger, M.R., Kane, H.J., Farquhar, G.D., 2006. Measurement of (carbon) kinetic isotope effect by Rayleigh fractionation using membrane inlet mass spectrometry for CO₂-consuming reactions. *Funct. Plant Biol.* 33 (12), 1115–1128.
- Mook, W.G., Bommeron, J.C., Staverman, W.H., 1974. Carbon isotope fractionation between dissolved bicarbonate and gaseous carbon dioxide. *Earth Planet. Sci. Lett.* 22, 169–176.
- Pagani, M., 2014. Biomarker-based inferences of past climate: the alkenone pCO₂ proxy. *Treatise on Geochemistry*, second ed.
- Pierrot, D., Lewis, E., Wallace, D.W.R., 2006. MS excel program developed for CO₂ system calculations. ORNL/CDIAC-105a. Carbon Dioxide Information Analysis Center, Oak Ridge National Laboratory, US Department of Energy, Oak Ridge, Tennessee.
- Price, G.D., Badger, M.R., Woodger, F.J., Long, B.M., 2008. Advances in understanding the cyanobacterial CO₂-concentrating-mechanism (CCM): functional components, C₃ transporters, diversity, genetic regulation and prospects for engineering into plants. *J. Exp. Bot.* 59 (7), 1441–1461.
- Ratti, S., Giordano, M., Morse, D., 2007. CO₂-concentrating mechanisms of the potentially toxic dinoflagellate *Protoceratium reticulatum* (*Dinophyceae*, *Gonyaulacales*). *J. Phycol.* 43 (4), 693–701.
- Raven, J.A., Johnston, A.M., 1991. Mechanisms of inorganic-carbon acquisition in marine phytoplankton and their implications for the use of other resources. *Limnol. Oceanogr.* 36, 1701–1714.
- Roeske, C.A., O'Leary, M.H., 1984. Carbon isotope effects on enzyme-catalyzed carboxylation of ribulose biphosphate. *Biochemistry* 23 (25), 6275–6284.
- Rost, B., Zondervan, I., Riebesell, U., 2002. Light dependent carbon isotope fractionation in the coccolithophorid *Emiliana huxleyi*. *Limnol. Oceanogr.* 47, 120–128.
- Rost, B., Riebesell, U., Burkhardt, S., Sültemeyer, D., 2003. Carbon acquisition of bloom-forming marine phytoplankton. *Limnol. Oceanogr.* 48 (1), 55–67.
- Rost, B., Richter, K.-U., Riebesell, U., Hansen, P.J., 2006. Inorganic carbon acquisition in red tide dinoflagellates. *Plant Cell Environ.* 29, 810–822.
- Rost, B., Kranz, S.A., Richter, K.-U., Tortell, P.D., 2007. Isotope disequilibrium and mass spectrometric studies of inorganic carbon acquisition by phytoplankton. *Limnol. Oceanogr. Methods* 5 (10), 328–337.
- Schulz, K.G., Riebesell, U., Rost, B., Thoms, S., Zeebe, R.E., 2006. Determination of the rate constants for the carbon dioxide to bicarbonate interconversion in pH-buffered seawater systems. *Mar. Chem.* 100, 53–65.
- Schulz, K.G., Rost, B., Burkhardt, S., Riebesell, U., Thoms, S., Wolf-Gladrow, D.A., 2007. The effect of iron availability on the regulation of inorganic carbon acquisition in the coccolithophore *Emiliana huxleyi* and the significance of cellular compartmentation for stable carbon isotope fractionation. *Geochim. Cosmochim. Acta* 71 (22), 5301–5312.
- Scott, K.M., Henn-Sax, M., Harmer, T.L., Longo, D.L., Frame, C.H., Cavanaugh, C.M., 2007. Kinetic isotope effect and biochemical characterization of form IA RubisCO from the marine cyanobacterium *Prochlorococcus marinus* MIT9313. *Limnol. Oceanogr.* 52 (5), 2199–2204.
- Sharkey, T.D., Berry, J.A., 1985. Carbon isotope fractionation of algae as influenced by an inducible CO₂ concentrating mechanism. In: Lucas, W.J., Berry, J.A. (Eds.), *Inorganic Carbon Uptake by Aquatic Photosynthetic Organisms*. The American Society of Plant Physiologists (ASPP), pp. 389–401.
- Silvermann, D.N., 1982. Carbonic anhydrase. Oxygen-18 exchange catalyzed by an enzyme with rate-contributing proton-transfer steps. *Methods Enzymol.* 87, 732–752.
- Trimborn, S., Wolf-Gladrow, D., Richter, K.U., Rost, B., 2009. The effect of pCO₂ on carbon acquisition and intracellular assimilation in four marine diatoms. *J. Exp. Mar. Biol. Ecol.* 376 (1), 26–36.
- Van de Waal, D.B., John, U., Ziveri, P., Reichart, G.J., Hoins, M., Slujs, A., Rost, B., 2013. Ocean acidification reduces growth and calcification in a marine dinoflagellate. *PLoS One* 8.
- Whitney, S.M., Andrews, T.J., 1998. The CO₂/O₂ specificity of single subunit ribulose biphosphate carboxylase from the dinoflagellate *Amphidinium carterae*. *Aust. J. Plant Physiol.* 25, 131–138.
- Zeebe, R.E., Wolf-Gladrow, D.A., 2001. *CO₂ in Seawater: Equilibrium, Kinetics, Isotopes*. Elsevier Science, Amsterdam, The Netherlands.